

Charge transfer cross sections for collisions of Li^{3+} , Be^{4+} , B^{5+} , and C^{6+} ions with atomic hydrogen

Hiroshi Ryufuku

Tokai Research Establishment, Japan Atomic Energy Research Institute, Tokai-mura, Naka-gun, Ibaraki 319-11 Japan

Tsutomu Watanabe*

Department of Applied Physics, Faculty of Engineering, The University of Tokyo, Bunkyo-ku, Tokyo 113 Japan

(Received 30 August 1978)

Charge transfer cross sections for $\text{Li}^{3+} + \text{H}$, $\text{Be}^{4+} + \text{H}$, $\text{B}^{5+} + \text{H}$, and $\text{C}^{6+} + \text{H}$ collisions are calculated for ion-impact energies from 0.025 to 200, or to 2000 (for the $\text{C}^{6+} + \text{H}$ case) keV/amu by means of the previously proposed unitarized formula based on the distorted-wave Born approximation. The results, compared with other theoretical and experimental values, show that the present formula is very useful for impact energies from 2 to 100 keV/amu, but tends to overestimate cross sections for impact energies greater than 100 keV/amu. It is suggested that the formula can be improved by taking direct-excitation and ionization channels into consideration. A scaling rule based on the cross section obtained by means of the present method is also considered, and is applied to scaling of the experimental data.

I. INTRODUCTION

Charge transfer processes between heavy multi-charged ions and hydrogen atoms have recently received appreciable attention, not only theoretically but also in connection with the heating of Tokamak fusion plasmas by neutral hydrogen-beam injection. Heavy-ion impurities in a confined plasma can reduce the penetration of the energetic neutral hydrogen beams as a result of electron capture from the hydrogen atoms. Thus the cross sections for electron capture from hydrogen atoms by highly stripped ions such as carbon, oxygen, silicon, molybdenum, tungsten, etc., which are present in Tokamak plasmas, are required for H-impact energies of 1–200 keV. For this reason, a program to estimate the cross sections for electron capture from hydrogen atoms by completely stripped ions of the above elements has been undertaken.

In a previous paper¹ (hereafter referred to as I), a unitarized distorted wave approximation (UDWA) method and an absorption model were applied to calculations of the charge transfer cross sections for collisions of O^{8+} with H, since the need for obtaining information on this process was of highest priority among the heavy-ion-hydrogen-atom reactions. The results showed reasonable agreement with the cross sections obtained by other workers. In particular, the UDWA results showed excellent agreement with some preliminary results of a molecular state calculation of Salop and Olson² and with the results of a classical trajectory calculation of those of Salop and Olson³ over the entire energy range considered by these authors. They used the method of closely coupled molecular states in the lower-energy range for

$E = 0.05\text{--}8$ keV/amu and the classical trajectory Monte Carlo method in the higher-energy range for $E = 37.5\text{--}150$ keV/amu. It is expected on the basis of the theory that the present method is applicable for energies greater than about 10 keV/amu. However, it is theoretically obscure as to whether the present method always gives results similar to those based on molecular calculations even below 1 keV/amu. For this reason, it is interesting to test the present method on many collisions involving other ions.

In the present work, the UDWA formula was applied to calculations of the charge transfer cross sections for collisions of the completely stripped ions, Li^{3+} , Be^{4+} , B^{5+} , and C^{6+} , with atomic hydrogen. The absorption model was also applied to the same reactions for comparison. The results are compared with experimental data for collisions of both completely and partially stripped ions and atomic hydrogen. At the present time, no experimental data are available for collisions of the completely stripped ions under consideration with atomic hydrogen, except for the data on $\text{Li}^{3+} + \text{H}$ and a single data point for $\text{B}^{5+} + \text{H}$. A scaling rule for these cross sections with respect to the value of the ionic charge Z was obtained using the UDWA results and was applied to the experimental cross sections.

Salop and Olson⁴ have reported charge transfer cross sections obtained using the Landau-Zener method for such collisions as $\text{C}^{6+} + \text{H}$, $\text{N}^{7+} + \text{H}$, $\text{O}^{8+} + \text{H}$, $\text{Ne}^{10+} + \text{H}$, $\text{Si}^{14+} + \text{H}$, and $\text{Ar}^{18+} + \text{H}$. Bottcher⁵ has attempted to estimate the charge transfer cross sections using a specified formulation of the interaction matrix with a basis set of stationary atomic orbitals. It is already known that these two methods considerably underestimate the cross

sections.^{1,2,6-8}

Vaaben and Briggs⁸ have obtained charge transfer cross sections for $C^{6+} + H$ collisions using an eleven-molecular-state calculation. Harel and Salin⁹ have reported three-molecular-state calculations for charge transfer in $Be^{4+} + H$, $B^{5+} + H$, and $O^{8+} + H$ collisions. Later, Salop and Olson⁷ evaluated the charge transfer cross section for $C^{6+} + H$ collisions using a six-molecular-state calculation, and further studied the dependence of the cross sections, which are calculated with molecular bases, on the coordinate origin. The classical trajectory Monte Carlo calculations of Olson and Salop³ also included charge transfer cross sections for ionic charges $Z = 3-6$. Comparisons of all these results with the present calculations are shown in the present paper.

In Sec. II, the UDWA formulation is described from the point of view of emphasizing the approximations introduced into the formulation, and in Sec. III, the numerical results are given and discussed. Atomic units are used throughout the paper, unless otherwise stated.

II. FORMULATION

We will consider the collision of a nucleus B (mass M_B , charge Z_B) with a hydrogenlike atom consisting of nucleus A (mass M_A , charge Z_A) and an electron. The straight-line trajectory approximation is used for the relative motion of A and B , where the position vector \vec{R} of B relative to A is described as

$$\vec{R} = \vec{v}t + \vec{e}_x\rho, \quad (2.1)$$

and \vec{v} is the impact velocity, ρ the impact parameter, \vec{e}_x the unit vector perpendicular to \vec{v} in the collision plane, and t the time chosen so that at $t=0$ the two nuclei have a minimum separation. If we can obtain the probability $P(\rho)$ for a given process as a function of ρ , then the cross section can be calculated using

$$\sigma = 2\pi \int_0^\infty P(\rho)\rho d\rho. \quad (2.2)$$

The electronic wave function $\chi(\vec{r}, t)$ satisfies the Schrödinger equation

$$i \frac{\partial \chi(\vec{r}, t)}{\partial t} = \mathcal{H} \chi(\vec{r}, t), \quad (2.3)$$

with

$$\mathcal{H} = -\frac{1}{2} \Delta - (Z_A/r_A) - (Z_B/r_B), \quad (2.4)$$

where $r_A = |\vec{r}_A|$, $r_B = |\vec{r}_B|$, $r = |\vec{r}|$, and \vec{r}_A , \vec{r}_B , and \vec{r} are the position vectors of the electron relative to A , B , and the midpoint of A and B , respectively, and Δ is the Laplacian with respect to \vec{r} .

Letting the linearly independent basis set $\{\xi_n\}$, the elements of which depend on time and are not always mutually orthogonal except for $t \rightarrow \pm\infty$, be complete representing all states involved in the reactions under consideration, then we can express $\chi(\vec{r}, t)$ in terms of $\xi_n(\vec{r}, t)$ as

$$\chi(\vec{r}, t) = \sum_n a_n(t) \xi_n(\vec{r}, t), \quad (2.5)$$

where $a_n(t)$ is the expansion coefficient.

Substituting Eq. (2.5) into Eq. (2.3) and denoting the state vector $\{a_n(t)\}$ by $|\Psi(t)\rangle$, we obtain the following equation for $|\Psi(t)\rangle$:

$$i \frac{d}{dt} |\Psi(t)\rangle = H |\Psi(t)\rangle, \quad (2.6)$$

with

$$H = s^{-1}h, \quad (2.7)$$

where s and h are the matrices the elements of which are given by

$$h_{mn} = \left[\xi_m, \left(\mathcal{H} - i \frac{\partial}{\partial t} \right) \xi_n \right] \quad (2.8)$$

and

$$s_{mm} = (\xi_m, \xi_m), \quad (2.9)$$

and s^{-1} is the inverse matrix of s .

As described in I, the S matrix defined by

$$|\Psi(\infty)\rangle = S |\Psi(-\infty)\rangle \quad (2.10)$$

can be written as

$$S = \exp\left(-i \int_{-\infty}^{\infty} H^0 dt\right) S^{\text{int}} \quad (2.11)$$

with

$$S^{\text{int}} = T \exp\left[-i \int_{-\infty}^{\infty} \hat{H}^{\text{int}}(t) dt\right], \quad (2.12)$$

where T is the chronological ordering operator and

$$\hat{H}^{\text{int}}(t) = \exp\left(i \int_{-\infty}^t H^0 dt\right) H^{\text{int}} \exp\left(-i \int_{-\infty}^t H^0 dt\right) \quad (2.13)$$

and

$$H^{\text{int}} = H - H^0, \quad (2.14)$$

where H^0 is the diagonal part of the matrix H , composed of the elements

$$\langle m | H^0 | n \rangle = \langle m | H | n \rangle \delta_{mn}. \quad (2.15)$$

The probability that the electron which was in the initial state $|0\rangle$ at $t = -\infty$ is found in the final state at $t = \infty$, is given by

$$P_{n_0}(\rho) = |\langle n | S | 0 \rangle|^2 \quad (2.16)$$

$$= |\langle n | S^{\text{int}} | 0 \rangle|^2. \quad (2.17)$$

Up to this point the only approximation which has been introduced into our formulation is the

$$\begin{aligned} \langle n | S^{\text{int}} | 0 \rangle &= \delta_{n_0} + \frac{-i}{1!} \int_{-\infty}^{\infty} \langle n | \hat{H}^{\text{int}}(t) | 0 \rangle dt + \frac{(-i)^2}{2!} \sum_k \int_{-\infty}^{\infty} \langle n | \hat{H}^{\text{int}}(t) | k \rangle dt \int_{-\infty}^{\infty} \langle k | \hat{H}^{\text{int}}(t) | 0 \rangle dt \\ &+ \frac{(-i)^3}{3!} \sum_k \sum_l \int_{-\infty}^{\infty} \langle n | \hat{H}^{\text{int}}(t) | k \rangle dt \int_{-\infty}^{\infty} \langle k | \hat{H}^{\text{int}}(t) | l \rangle dt \int_{-\infty}^{\infty} \langle l | \hat{H}^{\text{int}}(t) | 0 \rangle dt + \dots \end{aligned} \quad (2.18)$$

The second approximation is to neglect all matrix elements except those involving the initial state $|0\rangle$. These approximations are considered to be valid for processes at impact velocity so that $v \geq 1$. Using the second approximation in Eq. (2.18) and considering $\langle 0 | \hat{H}^{\text{int}}(t) | 0 \rangle = 0$, we obtain

$$\langle 0 | S^{\text{int}} | 0 \rangle = \cos p^{1/2} \quad (2.19)$$

and

$$\langle n | S^{\text{int}} | 0 \rangle = -it_{n_0} p^{-1/2} \sin p^{1/2}, \quad (2.20)$$

where

$$p = \sum_n |t_{n_0}|^2 \quad (2.21)$$

and

$$t_{n_0} = \int_{-\infty}^{\infty} \langle n | \hat{H}^{\text{int}}(t) | 0 \rangle dt. \quad (2.22)$$

It is clear from Eqs. (2.19), (2.20), and (2.21) that

$$\sum_n |\langle n | S^{\text{int}} | 0 \rangle|^2 = 1, \quad (2.23)$$

that is, the unitarity of S^{int} is not broken in the approximate formulas given by Eqs. (2.19)–(2.22).

Now we will consider how to determine the bases $\{\xi_n\}$ in Eq. (2.5). The processes to be considered in this problem are excitation, ionization, and charge transfer. From the fact that excitation and charge transfer result mainly in low-lying bound states of the atomic system, $A + \text{electron}$ and $B + \text{electron}$, respectively, and that ionization also results mainly in low-energy continuum states, we can cut off states having energy levels greater than an appropriate value. Thus we can use the following truncated set of bases to represent the initial and final states nearly completely.

$$\xi_n^A(\vec{r}, t) = \phi_n^A(\vec{r}_A) e^{-i\vec{v} \cdot \vec{r}/2} \quad (n=1, 2, 3, \dots, N_A), \quad (2.24)$$

$$\xi_n^B(\vec{r}, t) = \phi_n^B(\vec{r}_B) e^{i\vec{v} \cdot \vec{r}/2} \quad (n=1, 2, 3, \dots, N_B), \quad (2.25)$$

and

straight-line trajectory approximation which is valid except for very low impact processes.¹⁰

The first significant approximation in this treatment is to drop the chronological ordering operator T . Then, $\langle n | S^{\text{int}} | 0 \rangle$ can be expressed as

$$\xi_n^C(\vec{r}, t) = \begin{cases} \psi_n^A(\vec{r}_A) e^{-i\vec{v} \cdot \vec{r}/2} & (Z_A > Z_B), \\ \psi_n^B(\vec{r}_B) e^{i\vec{v} \cdot \vec{r}/2} & (Z_A < Z_B), \end{cases} \quad (2.26)$$

where $n=1, 2, 3, \dots, N_C$ and $\phi_n^A(\vec{r}_A)$ and $\phi_n^B(\vec{r}_B)$ are hydrogenlike wave functions of the system $A + \text{electron}$ and $B + \text{electron}$ having negative eigenenergies ω_n^A and ω_n^B , respectively, and $\psi_n^A(\vec{r}_A)$ and $\psi_n^B(\vec{r}_B)$ are those having positive eigenenergies. In Eqs. (2.26) and (2.27), a discrete index n is used for convenience instead of a continuous index. The time dependence of ξ_n^A , ξ_n^B , and ξ_n^C is represented by the positions of nuclei A and B . N_A , N_B , and N_C are the appropriate cutoff indices. At $t \rightarrow \pm\infty$ it is clear that $\{\xi_n^A, \xi_n^B, \xi_n^C\}$ is an orthogonal set of functions, while at finite internuclear separation it is not orthogonal. Except for low-energy impact processes, we can use the set $\{\xi_n^A, \xi_n^B, \xi_n^C\}$ for $\{\xi_n\}$ in Eq. (2.5) without introducing serious errors.

Using the bases defined in Eqs. (2.24), (2.25), (2.26), and (2.27) in Eq. (2.22), and using Eqs. (2.17) and (2.20)–(2.22), we obtain the charge transfer probability as follows:

$$P(\rho) = \frac{p_{CT}}{p_t} \sin^2 p_t^{1/2} \quad (2.28)$$

with

$$p_t = p_{CT} + p_{\text{exci}} + p_{\text{ion}}, \quad (2.29)$$

where

$$p_{CT} = \sum_{n=1}^{N_B} \left| \int_{-\infty}^{\infty} \langle n, B | \hat{H}^{\text{int}}(t) | 0, A \rangle dt \right|^2, \quad (2.30a)$$

$$p_{\text{exci}} = \sum_{n=1}^{N_A} \left| \int_{-\infty}^{\infty} \langle n, A | \hat{H}^{\text{int}}(t) | 0, A \rangle dt \right|^2, \quad (2.30b)$$

and

$$p_{\text{ion}} = \sum_{n=1}^{N_C} \left| \int_{-\infty}^{\infty} \langle n, C | \hat{H}^{\text{int}}(t) | 0, A \rangle dt \right|^2. \quad (2.30c)$$

Here $|0, A\rangle$ denotes the initial state, and Eqs. (2.30a), (2.30b), and (2.30c) express the probabilities based on the first-order approximation to the

S matrix [see Eq. (2.18)] for charge transfer, direct excitation, and ionization, respectively.

The third approximation in this treatment is to ignore the direct excitation and ionization channels. Then, the basis set becomes $\{\xi_0^A, \xi_n^B; n=1, 2, 3, \dots, N_B\}$ and Eq. (2.28) becomes

$$p(\rho) = \sin^2 p_{CT}^{1/2}. \quad (2.31)$$

$$S^{-1} = \frac{1}{1 - \sum_k |S_{0k}^{AB}|^2} \begin{bmatrix} 1 & -S_{01}^{AB} & -S_{02}^{AB} & -S_{03}^{AB} & \dots \\ -S_{10}^{BA} & 1 - \sum_{k \neq 1} |S_{0k}^{AB}|^2 & S_{10}^{BA} S_{02}^{AB} & S_{10}^{BA} S_{03}^{AB} & \dots \\ -S_{20}^{BA} & S_{20}^{BA} S_{01}^{AB} & 1 - \sum_{k \neq 2} |S_{0k}^{AB}|^2 & S_{20}^{BA} S_{03}^{AB} & \dots \\ -S_{30}^{BA} & S_{30}^{BA} S_{01}^{AB} & S_{30}^{BA} S_{02}^{AB} & 1 - \sum_{k \neq 3} |S_{0k}^{AB}|^2 & \dots \\ \dots & \dots & \dots & \dots & \dots \end{bmatrix}, \quad (2.32)$$

where

$$s_{mn}^{\alpha\beta} = (\xi_m^\alpha, \xi_n^\beta). \quad (2.33)$$

Then, by a straightforward calculation using Eqs. (2.7)–(2.9), (2.14), and (2.15) in Eq. (2.13), we can write $\langle n, B | \hat{H}^{\text{int}}(t) | 0, A \rangle$ in Eq. (2.30a) as

$$\langle n, B | \hat{H}^{\text{int}}(t) | 0, A \rangle = \left(h_{n0}^{BA} - s_{n0}^{BA} \frac{h_{00}^{AA} - \sum_k S_{0k}^{AB} h_{k0}^{BA}}{1 - \sum_k |S_{0k}^{AB}|^2} \right) \exp \left[i \int_{-\infty}^t \left(h_{nn}^{BB} - s_{n0}^{BA} \frac{h_{0n}^{AB} - \sum_k S_{0k}^{AB} h_{kn}^{BB}}{1 - \sum_k |S_{0k}^{AB}|^2} - \frac{h_{00}^{AA} - \sum_k S_{0k}^{AB} S_{k0}^{BA}}{1 - \sum_k |S_{0k}^{AB}|^2} \right) dt \right], \quad (2.34)$$

where

$$h_{nm}^{\alpha\beta} = \left[\xi_m^\alpha, \left(3C - i \frac{\partial}{\partial t} \right) \xi_n^\beta \right]. \quad (2.35)$$

It is reasonable to consider that terms including two or more off-diagonal elements of matrices s and h are always negligible, because the translational factor $\exp(-i\vec{v} \cdot \vec{r}/2)$ becomes a significant at high collision energies and because charge transfer cross sections result mostly from the comparatively large impact-parameters at low colli-

sion energies. Thus we obtain

$$\langle n, B | \hat{H}^{\text{int}}(t) | 0, A \rangle \simeq (h_{n0}^{BA} - s_{n0}^{BA} h_{00}^{AA}) \exp \left[i \int_{-\infty}^t (h_{nn}^{BB} - h_{00}^{AA}) dt \right]. \quad (2.36)$$

Using Eqs. (2.4), (2.35), and (2.36) in Eq. (2.30a), p_{CT} can be rewritten as

$$p_{CT} \simeq \sum_n |\langle n, B | T^{\text{DWBA}} | 0, A \rangle|^2 \quad (2.37)$$

with

$$\langle n, B | T^{\text{DWBA}} | 0, A \rangle = \int_{-\infty}^{\infty} dt (u_{n0}^{BA} - s_{n0}^{BA} u_{00}^{AA}) \exp \left[i \int_{-\infty}^t (\omega_n^B - \omega_0^A + u_{nn}^{BB} - u_{00}^{AA}) dt \right], \quad (2.38)$$

where

$$u_{n0}^{BA} = \left[\xi_n^B, \left(-\frac{Z_B}{r_B} \right) \xi_0^A \right], \quad (2.39a)$$

$$u_{nn}^{BB} = \left[\xi_n^B, \left(-\frac{Z_A}{r_A} \right) \xi_n^B \right], \quad (2.39b)$$

$$u_{00}^{AA} = \left[\xi_0^A, \left(-\frac{Z_B}{r_B} \right) \xi_0^A \right], \quad (2.39c)$$

and

$$s_{n0}^{BA} = (\xi_n^B, \xi_0^A). \quad (2.39d)$$

It is reasonable to conclude that, on the basis of the previous condition, the summation over n in Eq. (2.37) is carried out with respect to the truncated set of bases given by Eq. (2.25). However, since the convergence of the summation is so rapid, the numerical result is almost the same

regardless of whether the truncated set or the complete set is used.

Equation (2.38) shows the semiclassical distorted-wave Born approximation (DWBA) formula for the charge transfer amplitude which is equivalent to that Bates has derived using the two-state approximation.¹¹ In the framework in which the excitation and ionization channels are closed, such as that described above, Eq. (2.31) is consistent with the unitarity of S^{int} expressed in Eq. (2.23), since $\langle 0 | S^{\text{int}} | 0 \rangle$ is now given by $\cos p_{\text{CT}}^{1/2}$. Thus this treatment is characterized by an approximation that results in a unitarized expression for the S matrix based on the distorted-wave approximation. Therefore, this treatment is called the "UDWA".

Bottcher⁵ has also developed a unitary approximation to the S matrix. However, his formula is very different from the present formula with respect to the following points. Bottcher has (i) used stationary atomic bases instead of the moving atomic bases used in the present work and, consequently, momentum transfer was neglected; (ii) used atomic wave functions rotating with the line through the nuclei, instead of those with the quantization axis fixed along the direction of impact as in the present formula, and with no account taken of rotational coupling; (iii) neglected the off-diagonal elements of the matrix s defined by Eq. (2.9), which result from the nonorthogonality of the bases and which are important in the atomic-basis formulation; (iv) ignored the energy difference between the initial- and final-atomic states which is not negligibly small for charge transfer processes involving high- Z heavy ions.

Approximations (ii)–(iv) are very serious even at the low energies at which Bottcher applied the theory. As was shown in I for $\text{O}^{8+} + \text{H}$ collisions, his results are considerably different from the values obtained using the present formula with respect to the magnitude and energy dependence of the cross sections.

III. NUMERICAL RESULTS AND DISCUSSION

Cross sections were calculated for charge transfer from $H(1s)$ to Li^{3+} , Be^{4+} , B^{5+} , and C^{6+} for ion-impact energies of 0.025–2000 keV/amu for C^{6+} impact and 0.025–200 keV/amu for impact of the other ions. The calculations were carried out as described below.

The DWBA probabilities $\{p_n\}$ for charge transfer to all states having principal quantum number n were given by

$$p_n = \sum_{l=0}^{n-1} \sum_{m=-l}^l |\langle nlm, B | T^{\text{DWBA}} | 1s, H^+ \rangle|^2, \quad (3.1)$$

TABLE I. Values of n_{max} for $\text{Li}^{3+} + \text{H}$, $\text{Be}^{4+} + \text{H}$, $\text{B}^{5+} + \text{H}$, and $\text{C}^{6+} + \text{H}$ collisions.

Impact energy (keV/amu)	Li^{3+}	Be^{4+}	B^{5+}	C^{6+}
≥ 25	6	6	7	8
10	6	6	6	7
5	5	5	5	5
2.5			5	5
2	5	5		
1	5	4	5	5
≤ 0.5	4	4	5	5

where l and m denote the angular quantum numbers and B stands for Li^{3+} , Be^{4+} , B^{5+} , or C^{6+} , and T^{DWBA} is defined in Eq. (2.38). However, the numerical calculation of Eq. (3.1) was carried out only for n up to n_{max} which is shown in Table I. For n greater than n_{max} , p_n was estimated by the extrapolation procedure described in I. The ratios of the UDWA cross section without extrapolation, σ'_{UDWA} , to that with extrapolation, σ_{UDWA} , are also shown in Table II. The calculated UDWA cross sections are shown in Table III.

The DWBA probabilities p obtained by summing p_n over n are given in Figs. 1–5. For impact energies up to 5 keV/amu, the DWBA probabilities p correspond mainly to impact parameters smaller than 3.2, 7.7, 4.5, and 8.0 a.u., respectively, for impact of Li^{3+} , Be^{4+} , B^{5+} , and C^{6+} . These impact parameters correspond to the $n=2, 3, 3,$ and 4 shells, respectively. For impact energies greater than 5 keV/amu, the behavior of the DWBA probabilities for impact of Li^{3+} and B^{5+} are different from those for impact of Be^{4+} and C^{6+} . In the former cases, larger contributions from the higher-energy states, that is, $n=3$ and 4, respectively, than referred to above are clearly seen.

The UDWA cross sections are also shown in

TABLE II. Ratios of the UDWA cross section without extrapolation to that with extrapolation for $\text{Li}^{3+} + \text{He}$, $\text{Be}^{4+} + \text{H}$, $\text{B}^{5+} + \text{H}$, and $\text{C}^{6+} + \text{H}$ collisions.

Impact energy (keV/amu)	Li^{3+}	Be^{4+}	B^{5+}	C^{6+}
2000				4.04(-2) ^a
700				1.42(-1)
400				2.07(-1)
200	1.70(-1)	2.55(-1)	2.66(-1)	2.70(-1)
100	1.81(-1)	2.61(-1)	2.65(-1)	2.65(-1)
75	1.60(-1)	2.32(-1)	2.28(-1)	2.19(-1)
50	1.07(-1)	1.57(-1)	1.41(-1)	1.30(-1)
25	1.69(-2)	2.26(-2)	1.40(-2)	8.51(-3)
10	3.98(-5)	2.43(-5)	8.95(-5)	

^a 4.04(-2) denotes 4.04×10^{-2} .

TABLE III. UDWA cross sections for charge transfer in $\text{Li}^{3+} + \text{H}$, $\text{Be}^{4+} + \text{H}$, $\text{B}^{5+} + \text{H}$, and $\text{C}^{6+} + \text{H}$ collisions.

Impact energy (keV/amu)	Li^{3+}	Be^{4+}	B^{5+}	C^{6+}
2000				$1.12(-20)^a$
700				$1.29(-18)$
400				$1.42(-17)$
200	$2.73(-17)$	$6.08(-17)$	$1.10(-16)$	$1.76(-16)$
100	$2.19(-16)$	$4.29(-16)$	$6.94(-16)$	$1.00(-15)$
75	$4.09(-16)$	$7.51(-16)$	$1.16(-15)$	$1.63(-15)$
50	$7.76(-16)$	$1.30(-15)$	$1.88(-15)$	$2.52(-15)$
25	$1.41(-15)$	$2.08(-15)$	$2.76(-15)$	$3.42(-15)$
10	$1.78(-15)$	$2.88(-15)$	$3.27(-15)$	$4.08(-15)$
5	$1.33(-15)$	$3.42(-15)$	$2.75(-15)$	$4.31(-15)$
2.5			$1.78(-15)$	$4.68(-15)$
2	$7.96(-16)$	$4.42(-15)$		
1	$8.42(-16)$	$4.90(-15)$	$1.39(-15)$	$5.06(-15)$
0.5	$7.91(-16)$	$5.02(-15)$	$1.19(-15)$	$4.92(-15)$
0.25			$1.55(-15)$	$4.54(-15)$
0.2	$8.05(-16)$	$5.40(-15)$		
0.1	$7.03(-16)$	$4.39(-15)$	$1.46(-15)$	$2.81(-15)$
0.05	$7.19(-16)$	$3.58(-15)$	$1.39(-15)$	$1.96(-15)$
0.025	$6.09(-16)$	$2.68(-15)$	$1.43(-15)$	$2.37(-15)$

^a $1.12(-20)$ denotes $1.12 \times 10^{-20} \text{ cm}^2$.

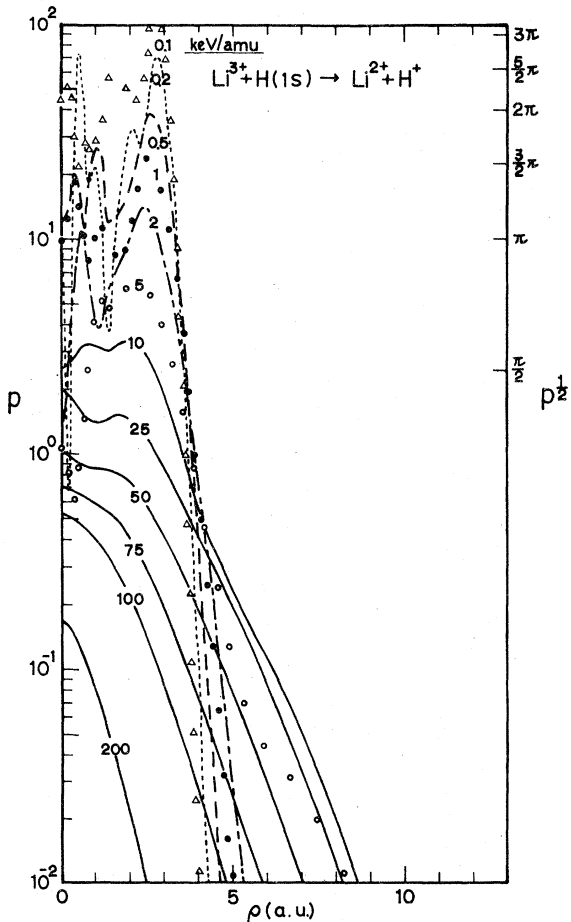


FIG. 1. DWBA probabilities p for the process $\text{Li}^{3+} + \text{H}(1s) \rightarrow \text{Li}^{2+} + \text{H}^+$ vs impact parameter ρ at impact energies from 0.1 to 200 keV/amu.

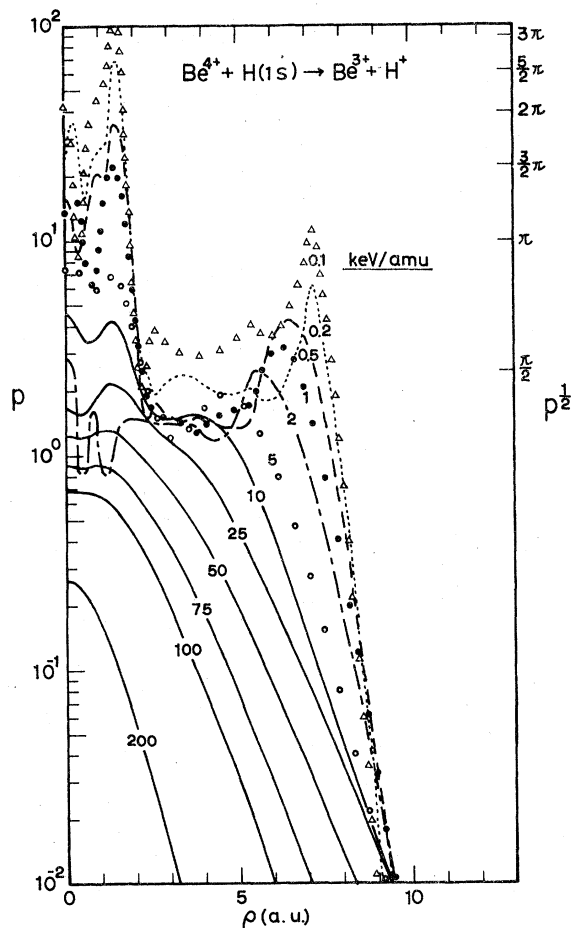


FIG. 2. Same as Fig. 1 for the process $\text{Be}^{4+} + \text{H}(1s) \rightarrow \text{Be}^{3+} + \text{H}^+$.

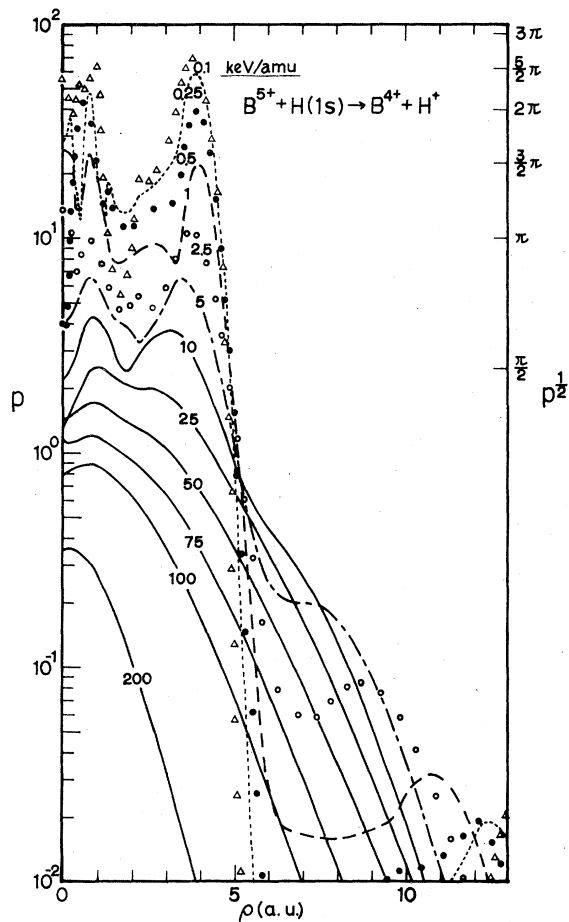


FIG. 3. Same as Fig. 1 for the process $B^{5+} + H(1s) \rightarrow B^{4+} + H^+$.

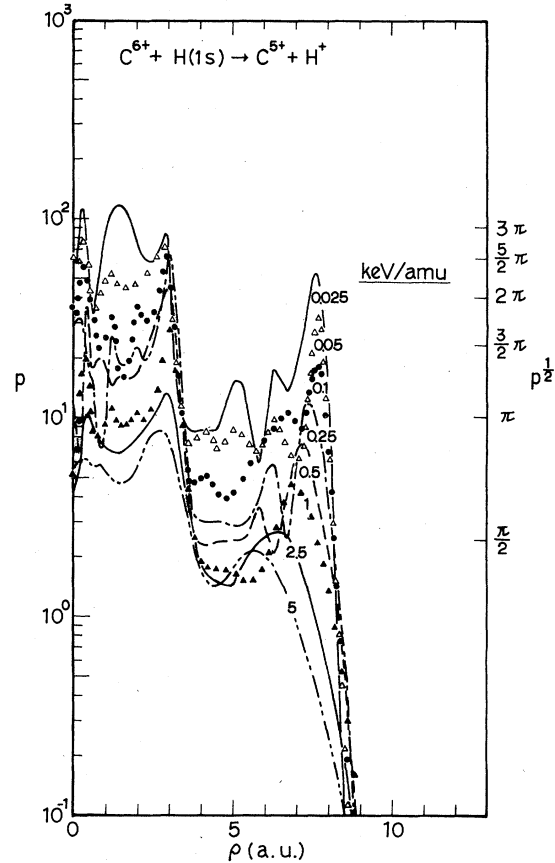


FIG. 4. Same as Fig. 1 for the process $C^{6+} + H(1s) \rightarrow C^{5+} + H^+$ and for impact energies from 0.025 to 5 keV/amu.

Figs. 6-9 with other theoretical results^{2,3,8,9,12} including those based on the absorption model, the theory of which has been reported in I, and data¹³⁻²⁰ for impact of ions of the same charge, as is indicated in the figures. The present results agree fairly well with the experimental data for impact energies greater than 3 keV/amu. For impact energies greater than about 100 keV/amu, the present results will decrease if the contribution from ionization channels is taken into consideration, as stated in Sec. II. Then agreement between the theoretical results and the experimental data would be better. The fact that the present theory tends to overestimate the charge transfer cross sections in the vicinity of 200 keV/amu is also confirmed from the data for impact of p on H and He^{2+} on H reported in I, and from the data obtained by Meyer *et al.*¹⁹ for impact of O^{8+} on H, which are the experimental results involving perhaps the highest Z bare nuclei available at the present time. The value found by the latter authors is 1.1

$\times 10^{-16}$ cm² at the impact velocity of 6×10^8 cm/sec (~ 200 keV/amu), which is about one-third of the value reported in I. Furthermore, the theoretical results obtained by Olson and Salop³ using the classical trajectory Monte Carlo method are smaller than the present values and closer to the experimental results including the O^{8+} -impact case, for impact energies between 100 and 200 keV/amu.

As shown in Fig. 8, the present results are closer to the data obtained by Crandall *et al.*²⁰ at impact energy of 6 keV/amu than are the other theoretical results. In comparison with the theoretical results for impact energies of 0.4-8 keV/amu in Fig. 8, the present results agree very well with those of Salop and Olson derived by placing the origin of the coordinate system on the proton. The fact that the present results approach their results with the origin on the proton rather than those with the origin on the projectile heavy ion is seen in all cases for which their theoretical results are available, that is, B^{5+} -, C^{6+} -, and

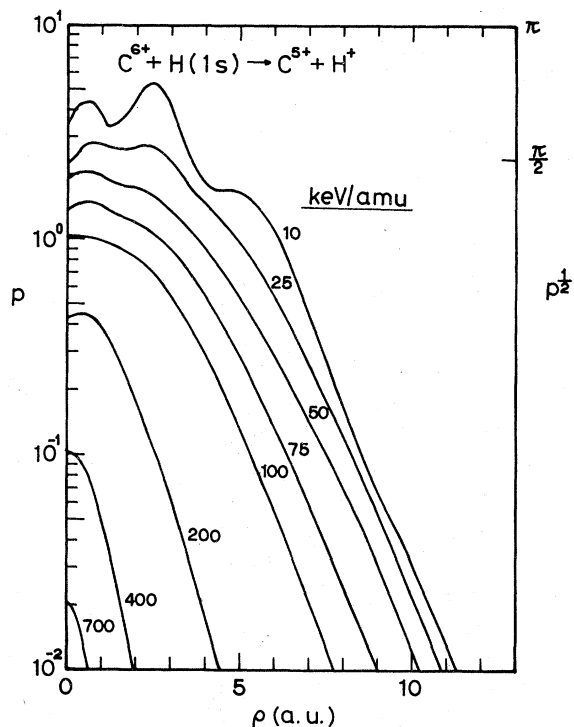


FIG. 5. Same as Fig. 4 for impact energies from 10 to 700 keV/amu.

O^{8+} -impact cases.^{2,7} In Figs. 8 and 9, the data obtained by Crandall *et al.*²⁰ for impact of partially stripped ions are seen to agree excellently with the theoretical results of Harel and Salin⁹ and of Vaaben and Briggs⁸ but, however, deviate from the present results. In Fig. 6, the theoretical results obtained by Olson *et al.*¹² for collisions of B^{3+} with H are shown, since no calculated results for low-energy impact of Li^{3+} on H are available. In Fig. 7, the results of Harel and Salin⁹ are very different from those reported here with respect to the energy dependence of the cross section.

As is shown in Figs. 6-9, in the low-energy region, the results derived using close-coupling methods based on molecular states, which are considered to be most applicable in this energy region, include non-negligible discrepancies, and the experimental results are not sufficient to determine the energy dependence of the cross sections. Therefore, no evaluation of the usefulness of the present theory in the low-energy region can be made. However, it becomes clear from the above that the present results connect smoothly to the results obtained by Salop and Olson⁷ and to some preliminary results obtained by Salop and Olson² with the origin placed on the proton, in the energy region of 1-10 keV/amu.

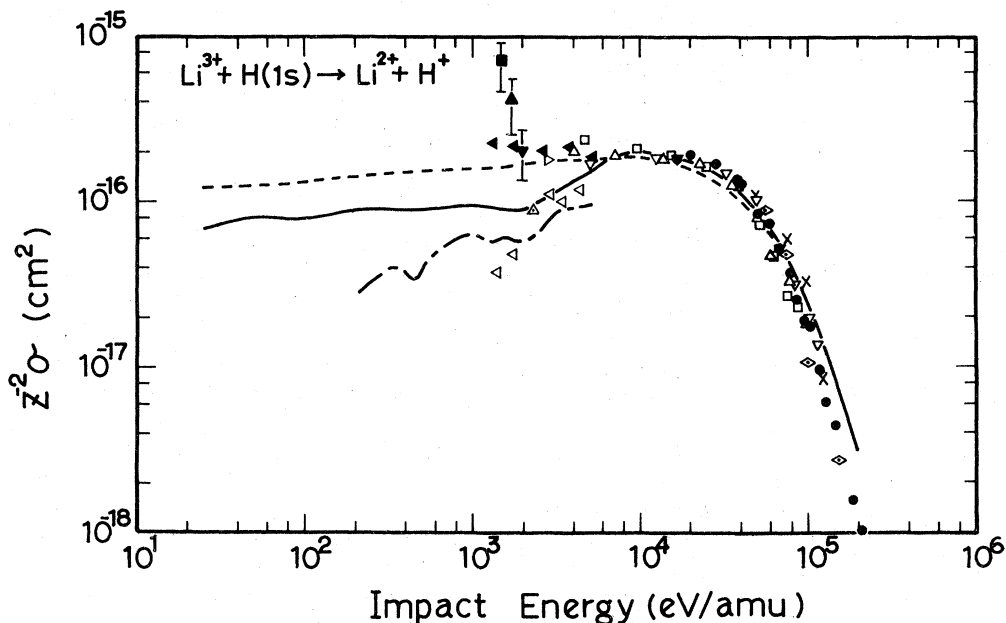


FIG. 6. Cross sections for the charge transfer process, $Li^{3+} + H(1s) \rightarrow Li^{2+} + H^+$, vs Li^{3+} -impact energy with $Z=3$. — denotes the present results, --- the absorption model, \times the results of Olson and Salop (Ref. 3; classical trajectory Monte Carlo method), and \bullet the experimental values of Shah *et al.* (Ref. 13). For comparison, also shown are the cross sections for electron capture from atomic hydrogen by partially stripped ions. — — — denotes the theoretical results of Olson *et al.* (Ref. 12) for B^{3+} -impact. Experimental results: ∇ (C^{3+}), Δ (N^{3+}), and \square (O^{3+}), Phaneuf *et al.* (Refs. 14 and 15); \blacktriangle (B^{3+}), \blacktriangledown (C^{3+}), \blacktriangle (N^{3+}), and \blacksquare (O^{3+}) Bayfield *et al.* (Ref. 18); \triangleleft (B^{3+}), \triangleright (C^{3+}), and \triangleleft (N^{3+}) Crandall *et al.* (Ref. 20); and \diamond (Si^{3+}) Kim *et al.* (Ref. 16).

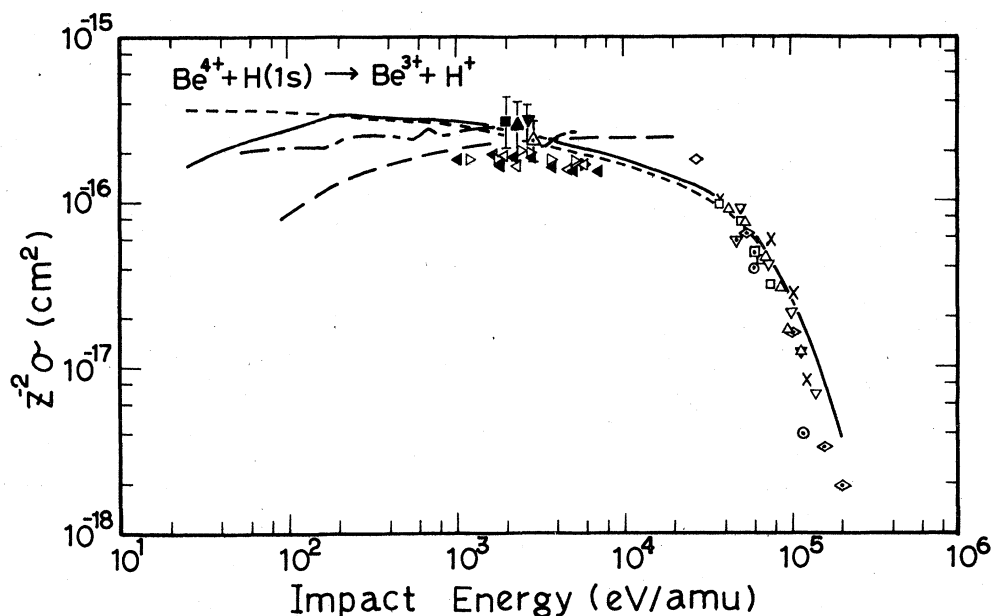


FIG. 7. Cross sections for the charge transfer process, $\text{Be}^{4+} + \text{H}(1s) \rightarrow \text{Be}^{3+} + \text{H}^+$, vs Be^{4+} -impact energy with $Z=4$. — denotes the present results, --- the absorption model, \times the results of Olson and Salop (Ref. 3; classical trajectory Monte Carlo method), and — — the results of Harel and Salin (Ref. 9; 3-molecular-state calculations). For comparison, also shown are the cross sections for electron capture from atomic hydrogen by partially-stripped ions. — — — denotes the theoretical results of Olson *et al.* (Ref. 12) for C^{4+} impact. Experimental results: ∇ (C^{4+}), Δ (N^{4+}), and \square (O^{4+}): Phaneuf *et al.* (Refs. 14 and 15) Δ (B^{4+}), ∇ (C^{4+}), \blacktriangle (N^{4+}), and \blacksquare (O^{4+}) Bayfield *et al.* (Ref. 18); \triangleleft (B^{4+}), \triangleright (C^{4+}), and \triangleleft (N^{4+}) Crandall *et al.* (Ref. 20); \diamond (Si^{4+}) Kim *et al.* (Ref. 16); \diamond (Fe^{4+}) Gardner *et al.* (Ref. 17); \circ (Fe^{4+}), \square (Mo^{4+}), and ∇ (W^{4+}) Meyer *et al.* (Ref. 19).

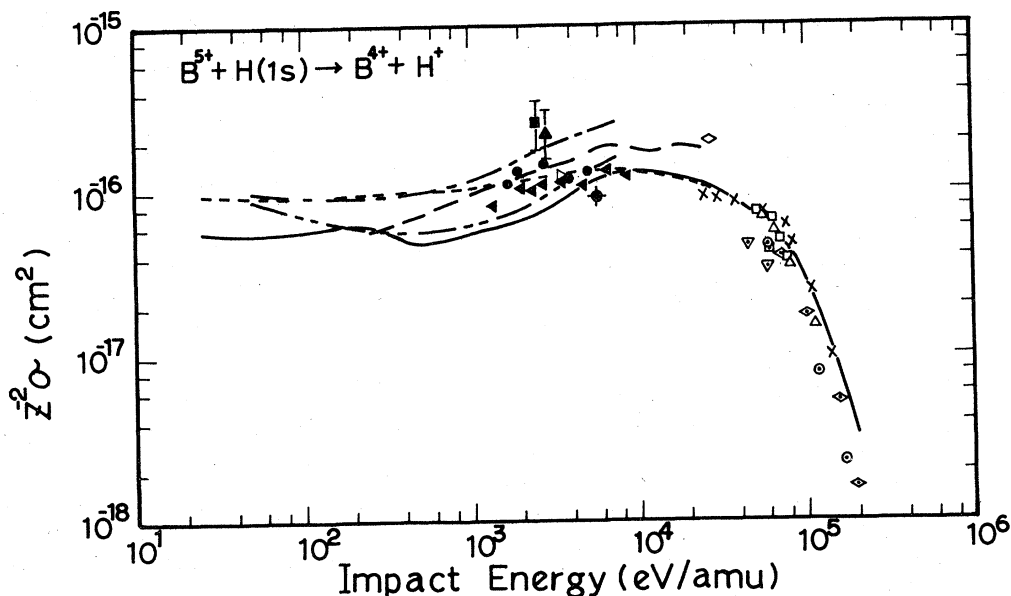


FIG. 8. Cross sections for the charge transfer process, $\text{B}^{5+} + \text{H}(1s) \rightarrow \text{B}^{4+} + \text{H}^+$, vs B^{5+} -impact energy with $Z=5$. — denotes the present results, --- the absorption model, \times the results of Salop and Olson (Ref. 3; classical trajectory Monte Carlo method), — — — and — — — the results of Salop and Olson (Ref. 2; 5-molecular-state calculations with the origin of the coordinates on B^{5+} and on H^+ , respectively), and — — — the results of Harel and Salin (Ref. 9; 3-molecular-state calculations). \blacklozenge shows the experimental value of Crandall *et al.* (Ref. 20). For comparison, also shown are experimental cross sections for electron capture from atomic hydrogen by partially stripped ions: Δ (N^{5+}) and \square (O^{5+}) Phaneuf *et al.* (Refs. 14 and 15); \blacktriangle (N^{5+}) and \blacksquare (O^{5+}) Bayfield *et al.* (Ref. 18); \triangleright (C^{5+}), \triangleleft (N^{5+}), and \bullet (O^{5+}) Crandall *et al.* (Ref. 20); \diamond (Si^{5+}) Kim *et al.* (Ref. 16); \diamond (Fe^{5+}) Gardner *et al.* (Ref. 17) and \circ (Fe^{5+}), \square (Mo^{5+}), and ∇ (W^{5+}) Meyer *et al.* (Ref. 19).

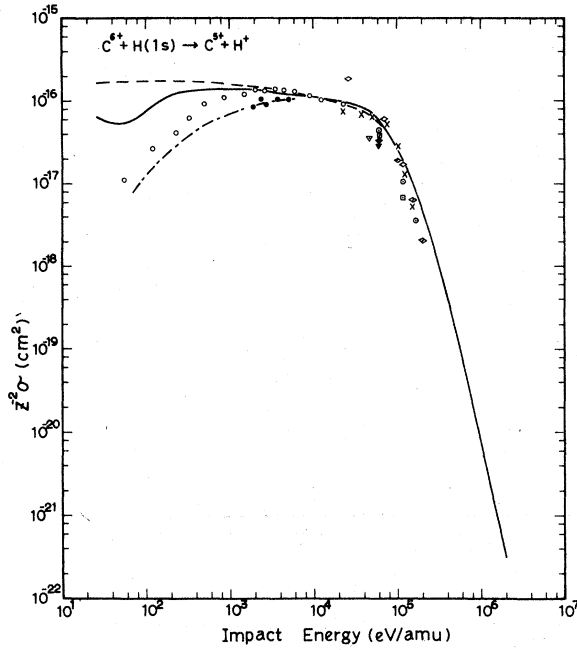


FIG. 9. Cross sections for the charge transfer process $C^{6+} + H(1s) \rightarrow C^{5+} + H^+$, vs C^{6+} -impact energy with $Z=6$. — denotes the present results, --- the absorption model, \times the results of Olson and Salop (Ref. 3; classical trajectory Monte Carlo method), \circ the results of Salop and Olson (Ref. 7; 6-molecular-state calculations with the origin of the coordinates on H^+) and — — the results of Vaaben and Briggs, (Ref. 8; 11-molecular-state calculations). For comparison, also shown are the experimental cross sections for electron capture from atomic hydrogen by partially stripped ions; \bullet (O^{6+}) Crandall *et al.* (Ref. 20); \diamond (Si^{6+}) Kim *et al.* (Ref. 16); \circ (Fe^{6+}) Gardner *et al.* (Ref. 17); and \square (Mo^{6+}), ∇ (W^{6+}), and \blacklozenge (Au^{6+}) Meyer *et al.* (Ref. 19).

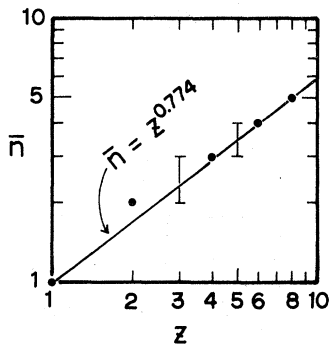


FIG. 10. Principal quantum number \bar{n} of the most probable state versus ionic charge Z for impact energies of 10–100 keV/amu. \square and \bullet denote UDWA results that with decreasing impact energy \bar{n} decreases from 3 to 2 for $Z=3$ and from 4 to 3 for $Z=5$, while it takes fixed values of 1, 2, 3, 4, and 5, respectively, for $Z=1, 2, 4, 6,$ and 8 .

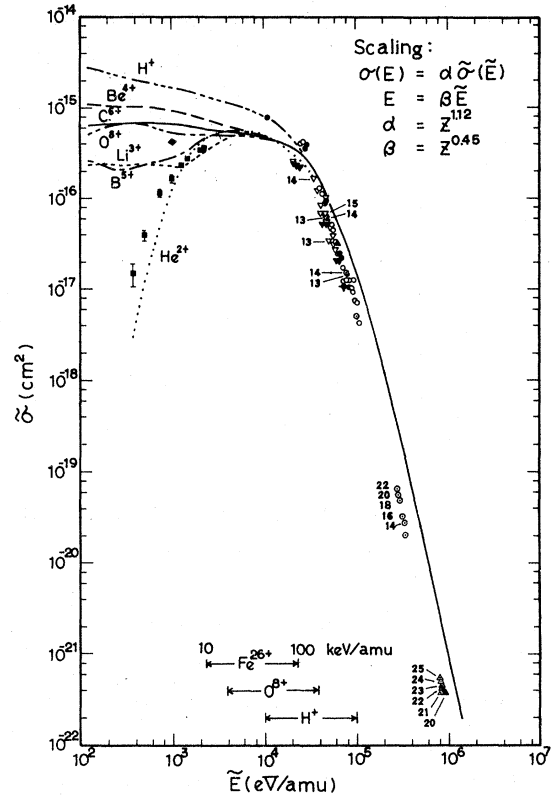


FIG. 11. Scaled cross sections $\tilde{\sigma}$ vs scaled impact energy \tilde{E} . The charge transfer cross sections and the impact energy are expressed as $\sigma(E) = \alpha \tilde{\sigma}(\tilde{E})$ and $E = \beta \tilde{E}$, respectively, with $\alpha = Z^{1.12}$ and $\beta = Z^{0.45}$. Also shown are the scaled experimental results: \blacksquare ($He^{2+} + H$) Nutt *et al.* (Ref. 21); \blacklozenge ($O^{8+} + H$) Meyer *et al.* (Ref. 19); \blacktriangleright ($Ar^{8+} + H$) Crandall *et al.* (Ref. 20); \bullet ($Fe^{7+ \sim 8+} + H$) and \circ ($Fe^{9+ \sim 13+} + H$) Gardner *et al.* (Ref. 17); \blacktriangle ($Si^{7+} + H$) Kim *et al.* (Ref. 16); \blacktriangledown ($Fe^{7+ \sim 8+} + H$) and ∇ ($Fe^{9+ \sim 15+} + H$) Meyer *et al.* (Ref. 19); \odot ($Fe^{9+ \sim 22+} + H_2$) Berkner *et al.* (Ref. 22); and \triangle ($Fe^{20+ \sim 25+} + H_2$) Berkner *et al.* (Ref. 23), where the numbers indicated express the value of ionic charge and the data for molecular-hydrogen targets denote one half the value of the measured cross sections.

Finally, scaling of the UDWA cross sections with respect to the ion charge Z will be considered on the basis of the results presented in this paper and those reported in I. Gardner *et al.*¹⁷ have found that the energy dependence of their data for $Fe^{Z+} (Z=4-13) + H$ collisions agrees well with that of the cross sections for $p + H$ collisions if the proton impact energy is doubled. Following this finding, an attempt was made to change the energy scale according to the energy state to which the electron is most probably transferred. As mentioned above, for impact energies of 10–100 keV/amu, the DWBA probabilities result mainly from final states having principal quantum

numbers $n=2-3$, 3 , $3-4$, and 5 , respectively, for ion charges of $Z=3$, 4 , 5 , 6 , and 8 . As a best-fit formula,

$$\bar{n} = Z^{0.774} \quad (3.2)$$

was obtained which gives $n=2.3$, 2.9 , 3.5 , 4.0 , and 5.0 corresponding to the respective Z values mentioned above (Fig. 10). Thus the scaling factor for the energy scale is determined as the ratio of the fictitious state energy corresponding to the principal quantum number \bar{n} to the $1s$ -state energy of a hydrogen atom, that is,

$$\beta = (Z/\bar{n})^2 = Z^{0.45}. \quad (3.3)$$

The impact energy E is scaled as

$$\tilde{E} = E/\beta. \quad (3.4)$$

Using the UDWA cross sections reported in this paper and I, the scaling factor for the cross section is determined to be

$$\alpha = Z^{1.12}. \quad (3.5)$$

The cross section σ is scaled as

$$\tilde{\sigma}(\tilde{E}) = \sigma(E)/\alpha, \quad (3.6)$$

where \tilde{E} is given by Eqs. (3.4) and (3.3).

The results are shown in Fig. 11 with the data obtained by Crandall *et al.*,²⁰ Gardner *et al.*,¹⁷ Nutt *et al.*,²¹ Kim *et al.*,¹⁶ Meyer *et al.*,¹⁹ and Berkner *et al.*^{22,23} It is of interest to apply the above scaling procedure to $Z > 8$. Some results are included in Fig. 11. The data plotted, including those for $Z \leq 8$, appear to fall along a single smooth curve. This is considered to give partial support to the applicability of the present scaling procedure

for high values of Z .

Further support comes from the use of the absorbing-sphere-model cross sections⁶ for high values of Z at low impact energies to estimate the scaling factor α . Using the absorbing-sphere model, the cross sections at low impact energies are evaluated as

$$\sigma_Z = \pi \left[\frac{2(Z-1)}{(Z/\bar{n})^2 - 1} \right]^2 = \pi \left[\frac{2(Z-1)}{\beta - 1} \right]^2 \quad (3.7)$$

$$\stackrel{Z \rightarrow \infty}{\approx} 4\pi (Z^2/\beta^2). \quad (3.8)$$

From this relation, we obtain

$$\alpha \propto Z^2/\beta^2 \quad (Z \rightarrow \infty). \quad (3.9)$$

If $\beta = Z^{0.45}$ is valid for high values of Z , we obtain $\alpha \propto Z^{1.10}$. The Z dependence of α is very close to that of Eq. (3.5). However, more precise theoretical investigations are necessary to clarify the problem.

ACKNOWLEDGMENTS

The authors would like to express their thanks to Dr. D. H. Crandall, Dr. F. W. Meyer, Dr. R. A. Phaneuf, Dr. H. J. Kim, Dr. P. Hvelplund, and Dr. P. H. Stelson, and also to Dr. J. E. Bayfield, Dr. P. M. Koch, Dr. L. D. Gardner, Dr. I. A. Sellin, Dr. D. J. Pegg, and Dr. R. S. Peterson for providing us with their experimental data prior to publication. Thanks are also due to Dr. W. Shearer-Izumi for careful reading of the manuscript, and to Miss Kayoko Hirai for her continual assistance in computation and in preparing of this paper.

*Present address through July 1979: FOM-Instituut voor Atoom- en Molecuulfysica, Kruislaan 407, Amsterdam, The Netherlands.

¹H. Ryufuku and T. Watanabe, Phys. Rev. A **18**, 2005 (1978).

²A. Salop and R. E. Olson (private communication).

³R. E. Olson and A. Salop, Phys. Rev. A **16**, 531 (1977).

⁴A. Salop and R. E. Olson, Phys. Rev. A **13**, 1312 (1976).

⁵C. Bottcher, J. Phys. B **10**, L213 (1977).

⁶R. E. Olson and A. Salop, Phys. Rev. A **14**, 579 (1976).

⁷A. Salop and R. E. Olson, Phys. Rev. A **16**, 1811 (1977).

⁸J. Vaaben and J. S. Briggs, J. Phys. B **10**, L521 (1977).

⁹C. Harel and A. Salin, J. Phys. B **10**, 3511 (1977).

¹⁰H. Ryufuku and T. Watanabe, J. Phys. Soc. Jpn. **41**, 991 (1976).

¹¹D. R. Bates, Proc. R. Soc. A **247**, 294 (1958).

¹²R. E. Olson, E. J. Shipsey, and J. C. Browne, J. Phys. B **11**, 699 (1978).

¹³M. B. Shah, T. V. Goffe, and H. B. Gilbody, J. Phys. B **11**, L233 (1978).

¹⁴R. A. Phaneuf, F. W. Meyer, R. H. McKnight, R. E. Olson, and A. Salop, J. Phys. B **10**, L425 (1977).

¹⁵R. A. Phaneuf, F. W. Meyer, and R. H. McKnight, Phys. Rev. A **17**, 534 (1978).

¹⁶H. J. Kim, R. A. Phaneuf, F. W. Meyer, and P. H. Stelson, Phys. Rev. A **17**, 854 (1978).

¹⁷L. D. Gardner, J. E. Bayfield, P. M. Koch, H. J. Kim, and P. H. Stelson, Phys. Rev. A **16**, 1415 (1977).

¹⁸J. E. Bayfield, P. M. Koch, L. D. Gardner, I. A. Sellin, D. J. Pegg, R. S. Peterson, and D. H. Crandall, *Contributed Papers of the International Conference on Atomic Physics*, edited by R. Marrus, M. H. Prior, and H. A. Shugart (Berkeley, California, 1976), p. 126; revised values in L. D. Gardner, Ph.D. dissertation (Yale University, 1978) (unpublished).

¹⁹F. W. Meyer, R. A. Phaneuf, H. J. Kim, P. Hvelplund, and P. H. Stelson, Phys. Rev. A (to be published).

²⁰D. H. Crandall, R. A. Phaneuf, and F. W. Meyer (private communication).

²¹W. L. Nutt, R. W. McCullough, K. Brady, M. B. Shah,
and H. B. Gilbody, *J. Phys. B* 11, 1457 (1978).

²²K. H. Berkner, W. G. Graham, R. V. Pyle, A. S.
Schlachter, J. W. Stearns, and R. E. Olson, *J. Phys.*

B 11, 875 (1978).

²³K. H. Berkner, W. G. Graham, R. V. Pyle, A. S.
Schlachter, and J. W. Stearns, *Phys. Lett. A* 62, 407
(1977).